

Towards First Detection of the Solar MSW Transition With JUNO

Obada Nairat  ^{1,2,*} John F. Beacom  ^{1,2,3,†} Kevin J. Kelly  ^{4,‡} and Shirley Weishi Li  ^{5,§}

¹*Center for Cosmology and AstroParticle Physics (CCAPP), Ohio State University, Columbus, OH 43210*

²*Department of Physics, Ohio State University, Columbus, OH 43210*

³*Department of Astronomy, Ohio State University, Columbus, OH 43210*

⁴*Department of Physics and Astronomy, Mitchell Institute for Fundamental Physics and Astronomy, Texas A&M University, College Station, TX 77843*

⁵*Department of Physics and Astronomy, University of California, Irvine, CA 92697*

(Dated: Jan 29, 2026)

Matter-induced neutrino flavor mixing (the Mikheyev-Smirnov-Wolfenstein, or MSW, effect) is a central prediction of the neutrino mixing framework, but it has not been conclusively observed. Direct observation of the energy-dependent MSW transition in the solar electron-neutrino survival probability would solve this, but backgrounds have been prohibitive. We show that our new technique for suppressing muon-induced spallation backgrounds will allow JUNO to measure the MSW transition at $>4\sigma$ significance in 10 years. This would strongly support upcoming multi-\$1B next-generation long-baseline experiments and their goals in cementing the neutrino mixing framework.

Introduction.— Neutrino flavor mixing in vacuum has been definitively established, showing that neutrinos have nonzero masses [1–12]. When neutrinos propagate through matter, their mixing can be substantially modified by the Mikheyev–Smirnov–Wolfenstein (MSW) effect [13, 14], which arises from coherent forward scattering via the weak interactions. Because these matter mixing effects depend on neutrino interactions at zero momentum transfer, they are highly sensitive to physics beyond the Standard Model (BSM) [15–32]. A quantitative experimental validation of matter mixing effects therefore remains an important goal.

However, no experiment has yet provided an unambiguous confirmation of matter mixing effects. For long-baseline and atmospheric experiments [33–37], it is challenging in part because Earth’s column density is small. For solar experiments, the large and varying density of the Sun offers a powerful laboratory [38–40]. *But while data on the electron-neutrino survival probability imply an MSW transition at a few MeV, it has never been directly observed [6, 10, 17, 19, 41].* Further, measurements of the solar day-night effect, which also probe the MSW theory, are similarly inconclusive [6, 41].

A precise understanding of matter mixing effects is crucial not only for fundamental physics, but also for practical reasons. First, the Deep Underground Neutrino Observatory (DUNE) long-baseline experiment seeks to measure the neutrino mass ordering and the CP-violating phase [42, 43]; these measurements either depend on matter effects or are vulnerable to degeneracies with BSM scenarios [44–47]. (The Tokai to Hyper-Kamiokande, or T2HK, long-baseline experiment will also seek to measure the CP-violating phase, but under minimal matter effects [48].) Second, matter effects will be important for high-statistics measurements of atmospheric neutrinos in DUNE, T2HK, and other experiments [28, 35, 49, 50]. Third, matter effects are essential for interpreting observations of supernova neutrinos [51–54].

In this *Letter*, we show that the Jiangmen Underground Neutrino Observatory (JUNO) [55–57] — de-

signed primarily to measure reactor neutrinos — can uniquely resolve this critical issue. In a companion paper [58], we present a powerful new background rejection technique for JUNO measurements of *solar neutrinos*. Exploiting this will give JUNO world-leading sensitivity to the MSW transition and will solidify the neutrino mixing framework. Figure 1 contrasts the current experimental status versus our projected sensitivity for JUNO.

Review of the MSW effect.— Neutrino mixing in vacuum can be described by a Hamiltonian evolution equation [40, 59, 60]. This depends upon the mixing angles between the flavor and mass eigenstate bases (θ_{ij}) and the mass-squared differences for the mass eigenstates (Δm_{ji}^2) [61]. When neutrinos propagate in matter, the Hamiltonian is modified by adding the MSW term (“the matter potential”) for electron neutrinos. This term is $\propto G_F N_e$, where G_F is the Fermi constant and N_e is the electron density in the medium [13, 14, 19, 28, 59, 60, 62]. For solar neutrinos of energy E_ν , the electron-neutrino survival probability is [19, 63]

$$P_{ee}(E_\nu) \simeq \sin^4(\theta_{13}) + \cos^4(\theta_{13}) P_{ee}^{2\nu}(E_\nu), \quad (1)$$

$$P_{ee}^{2\nu}(E_\nu) = \frac{1}{2}[1 + \cos(2\theta_{12})\langle \cos(2\theta_m) \rangle], \quad (2)$$

where $\cos(2\theta_m)$ refers to the matter mixing angle, and this term is averaged over the solar production region [64–67]. The energy dependence of Eq. (2) — which provides a direct probe of matter mixing effects — arises from θ_m , which depends on the vacuum mixing angle and a dimensionless quantity $\propto G_F N_e E_\nu / \Delta m_{21}^2$. The angle θ_m is θ_{12} in vacuum (or low neutrino energies), $\pi/4$ at the MSW resonance density (or energy), and $\pi/2$ at high density (or high neutrino energies).

Figure 1 shows the expected survival probability in the standard MSW framework using mixing parameters from the latest global fit [68] and recent JUNO measurements [57]. At the low energies probed by Borexino measurements (using pp , pep , and ${}^7\text{Be}$ neutrinos) [10], the results are consistent with the vacuum limit of Eq. (2).

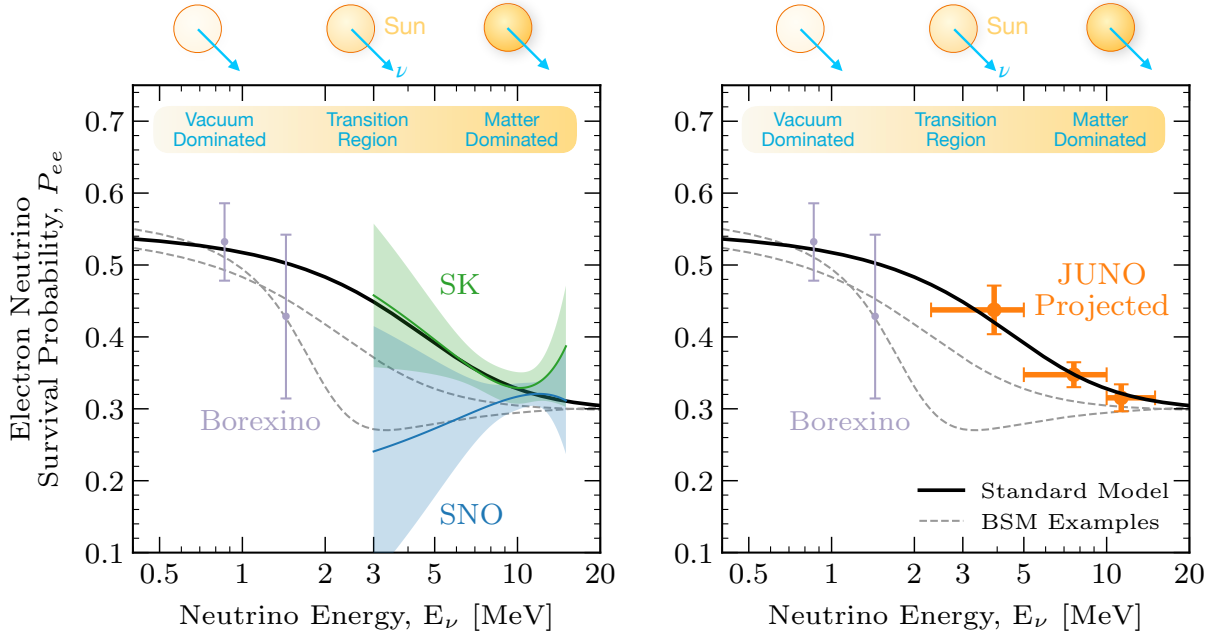


FIG. 1. Comparison of current [6, 10, 41] and projected measurements (using our background-rejection techniques for JUNO) of the solar MSW transition. The black line shows the MSW prediction, while the gray dashed lines show example allowed NSI models. The bins shown for JUNO are a projection, assuming the Standard Model, of how they could go beyond the quadratic fits used by SK and SNO. *With our spallation cuts, JUNO can measure the MSW transition well.*

At the high energies probed by Super-Kamiokande (SK) and Sudbury Neutrino Observatory (SNO), the results are consistent with the high-density limit [6, 41]. In the few-MeV transition region, limited statistics lead to large uncertainties: SK data weakly favor an *upturn* (at 1.2σ), while SNO data weakly favor a *downturn* (at 0.7σ). When taken together they somewhat favor an *upturn* (at 2.1σ) [4, 41]. These measurements are thus not yet sufficient to test matter mixing effects.

Figure 1 also shows that the survival probability can be modified by BSM physics, where we focus on non-standard interactions (NSI) induced by new heavy mediators [17, 19, 20, 22, 26–28, 30, 32, 40, 69–72]. Other possibilities include neutrino decay, sterile neutrinos, and large neutrino magnetic moments [15, 16, 18, 19, 21, 25]. For NSI, the matter potential is modified by new interactions between neutrinos and fermions, adding a new term that is $\propto G_F N_f \epsilon_{\alpha\beta}^f$, where N_f is the density of the fermion f in the medium and $\epsilon_{\alpha\beta}^f$ are dimensionless parameters that quantify the strength of the NSI between that fermion and the neutrino flavors ν_α and ν_β [20, 28]. We consider two example NSI models that are allowed at the 3σ level, corresponding to the parameters $(\epsilon_D, \epsilon_N) = (-0.20, -0.30)$ (bottom line) and $(-0.15, -0.12)$ (top line) as defined in Refs. [27, 29, 73]. These are equivalent to $\epsilon_{ee}^d \sim 0.4$ and $\epsilon_{e\tau}^d \sim 0.1$.

Prospects for solar neutrinos in JUNO.— Of present and planned detectors, JUNO has the best potential to make precise measurements of the MSW transition. (For comparison, Hyper-Kamiokande expects to have a sensitivity of 3σ in 10 years with an expected

threshold of 4.5 MeV but may do better [48, 50].) JUNO detects solar neutrinos through scattering with electrons, where the recoiling electron produces a prompt scintillation signal. The large scintillation light yield provides excellent energy resolution ($3\%/\sqrt{(E/\text{MeV})}$) and enables a low detection threshold [56, 57, 74], both essential for detecting the MSW transition. With a 20-kton target mass, nearly 70 times larger than Borexino, JUNO will detect ^8B neutrinos at a rate of ~ 80 events per day [56, 75].

JUNO’s analysis threshold for ^8B solar neutrinos is set by detector backgrounds. One important source is the natural radioactivity originating from contaminants in the scintillator or surrounding material. These backgrounds are effectively mitigated through multiple purification techniques and fiducial volume cuts [56]. Initial performance results [74] indicate that the concentrations of uranium and thorium in the detector are within the levels necessary to achieve a 2.3-MeV threshold, the lowest to date. A somewhat high activity rate of polonium may be a challenge, but it should fall to the required level within roughly one year, based on its 138.4-day half-life.

For the analysis window of 2.3–15 MeV, the dominant background is caused by the delayed decays of radioactive isotopes produced by cosmic-ray muons through spallation (nuclear breakup) processes [56, 58]. The rate of these decays is ~ 4000 events per day. The standard approach to reducing spallation backgrounds is to veto all events within a cylindrical region following a cosmic-ray muon. In Ref. [56], JUNO defined baseline cuts that would reduce spallation backgrounds to the sub-percent level, but at the cost of 50% signal loss.

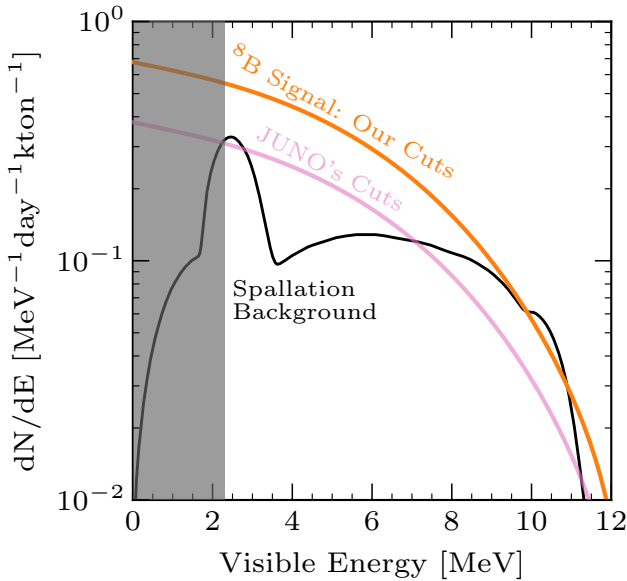


FIG. 2. The ${}^8\text{B}$ signal spectrum at JUNO using our neutron-tagged cuts compared to using JUNO’s cuts [56], both compared to the remaining spallation background spectrum. *With our spallation cuts, twice more signal would be retained.*

New technique to reduce backgrounds.— For JUNO to achieve its full potential as a solar neutrino detector, improved background rejection techniques are required. In earlier papers on SK [76–79], we showed that nearly all spallation isotopes are produced in muon-induced hadronic showers through the secondary particles associated with them, such as charged pions and neutrons. Importantly, hadronic showers are rare and are produced by $\lesssim 5\%$ of muons. These considerations are general to other detectors [58, 80]. This motivates a strategy with aggressive cuts on hadronic showers and moderate cuts on electromagnetic showers.

In a companion paper [58], we demonstrate that secondary neutrons are an efficient signature to tag hadronic showers in JUNO. These neutrons scatter down to thermal energies and capture on hydrogen, emitting a 2.2 MeV gamma ray, which JUNO detects with nearly perfect efficiency. For hadronic showers, we find an average yield of ~ 14 neutrons, and at least one neutron 98% of the time. For hadronic showers, we apply cylindrical cuts with radii up to 6 m and times up to 40 s. For electromagnetic showers, we instead limit these to 3 m and 5 s. This strongly suppresses spallation backgrounds while keeping the deadtime (signal loss) minimal.

Figure 2 shows the increase in the ${}^8\text{B}$ signal rate at JUNO using our neutron-tagged cuts (for the details of this figure, see Ref. [58]). For the same background reduction efficiency, our method reduces the deadtime by a factor of ~ 5 compared to JUNO’s baseline approach (from $\sim 50\%$ to $\sim 10\%$), yielding a factor of ~ 2 gain in exposure. This improvement in the signal-to-background ratio is critical for testing the MSW transition.

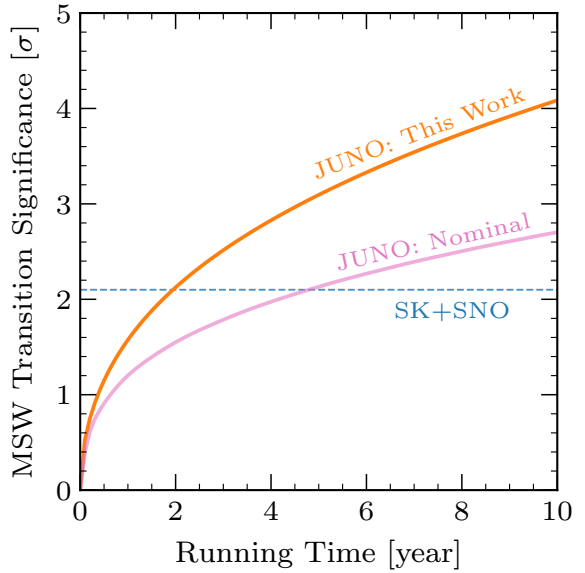


FIG. 3. Comparison of JUNO’s sensitivity to the solar MSW transition with our cuts and without, as well as to the combined SK+SNO result [41]. *With our spallation cuts, greater significance would be reached, and more quickly.*

Probing the MSW transition.— To test sensitivity to matter mixing effects, one must compare simulated data in JUNO under two hypotheses:

1. $P_{ee} = \text{constant}$ (but allowed to vary).
2. P_{ee} given by the MSW theory in Eq. (2).

With JUNO’s baseline cuts, they could reject the constant-probability hypothesis at 2.7σ significance in 10 years [56], somewhat better than the present combined SK+SNO result of 2.1σ .

We calculate the recoil electron spectrum for each case by convolving the ${}^8\text{B}$ neutrino spectrum [81] with the elastic neutrino-electron cross section, including radiative corrections [82], and the appropriate survival probability. There is a minor gain from the fact that the ${}^8\text{B}$ spectrum from Ref. [81] has reduced shape uncertainties compared to the one adopted in Ref. [56]. We incorporate detector effects, including the energy resolution ($\sim 3\%$ at 1 MeV) energy-scale uncertainty ($\sim 1\%$) [56, 74], detection efficiency [56], and fiducial volume cuts [56]. We simulate the detector backgrounds, including spallation isotopes, intrinsic radioactivities, and reactor neutrino elastic scattering [56]. We take into account statistical uncertainties as well as appreciable systematic uncertainties on the flux [6], spectrum shape [81], and backgrounds [56].

To quantify JUNO’s discrimination power, we follow the approach of their Ref. [56]. Assuming the MSW case as the truth and using bins of width 0.1 MeV, we evaluate the hypothesis of the flat-probability case using a χ^2 test, taking into account all uncertainties. Our analysis is slightly more conservative than JUNO’s, as we start at 2.3 MeV instead of 2.0 MeV to take into account a new spallation background we identified (see Ref. [58]).

Figure 3 shows that JUNO, with improved spallation cuts and assuming the Standard Model, can reject the flat survival probability hypothesis with $>4\sigma$ significance in 10 years. Moreover, JUNO will surpass the current SK+SNO result in about two years, less than half the time needed with JUNO’s baseline cuts. Of course, JUNO results may also favor BSM scenarios. This highlights the significance of our new background rejection techniques [58]. We expect that our results can be improved further by developing likelihood-based cuts and employing machine learning techniques [83, 84].

As an aside, in Fig. 1, we illustrate how JUNO could measure the survival probability in mostly uncorrelated bins, with different systematics dominating the uncertainties in each. This approach is in contrast to the quadratic fit bands used by SK and SNO. In calculating these bins, we follow Refs. [6, 41] in extracting the electron-neutrino survival probability by taking into account the contribution of muon and tau neutrinos.

Implications for future experiments.— Measurements of long-baseline neutrino flavor mixing aim to determine, among other goals, the neutrino mass ordering and the value of the CP-violating phase. At DUNE, the ability to perform these measurements is linked directly to the presence of matter effects. If BSM physics alters neutrino propagation in matter, it could pose significant challenges for these measurements. For example, NSI can substantially degrade the mass-ordering sensitivity [47, 69, 70, 72, 85–87] or even lead to errant interpretations of CP violation in long-baseline neutrino mixing [46, 88–91].

To quantify the impact of matter-effect degeneracies on DUNE’s mass-ordering reach, we simulate expected event rates (in electron- and muon-neutrino samples) assuming six years of data collection — equal running in neutrino and antineutrino modes — with a detector fiducial mass of 20 kton. Mixing parameters are fixed to the best-fit values from Ref. [68] (with solar parameters updated from Ref. [57]), with a varying assumed-true δ_{CP} . For the DUNE Baseline scenario, we allow θ_{23} , δ_{CP} , and Δm_{31}^2 (fixing $\Delta m_{31}^2 < 0$) to vary, obtaining a best-fit χ^2 .

We consider representative NSI scenarios where the additional effective electron neutrino coupling is $\epsilon_{ee} = \sum_f \epsilon_{ee}^f N_f / N_e$. Current global constraints on ϵ_{ee} are model-dependent and vary depending on the mediator mass, but allow values roughly in the range $(-1, 1)$ at the 3σ level [27, 28]. A precise measurement of the expected MSW transition in JUNO would restrict ϵ_{ee} to the range $(-0.2, 0.2)$ at 1σ and $(-0.3, 0.4)$ at 3σ .

Figure 4 illustrates how JUNO’s measurement of the MSW transition can mitigate degeneracies that affect DUNE’s sensitivity to the mass ordering. When all $\epsilon = 0$ (the Standard Model), DUNE will reach a significance of $7\text{--}15\sigma$, depending on the value of the CP-violating phase, δ_{CP} . Allowing NSI within currently allowed bounds introduces degeneracies that reduce this sensitivity to being below 5σ for the majority of δ_{CP} values, which would undermine DUNE’s goals. However, by independently

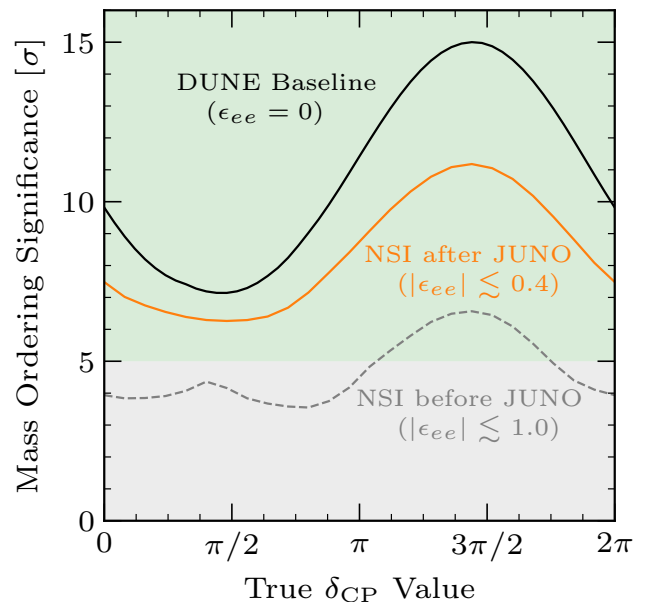


FIG. 4. DUNE sensitivity to the neutrino mass ordering under different assumptions: Standard Model only, NSI within a currently allowed range, and NSI constrained by JUNO’s measurement of the MSW transition. *JUNO’s measurement of matter mixing effects will support DUNE’s success.*

probing matter mixing effects through solar neutrinos, JUNO will lift these degeneracies and restore DUNE’s mass-ordering sensitivity to more than 5σ for all δ_{CP} .

Conclusions.— We have shown that JUNO can provide a decisive experimental test of the MSW transition in solar neutrino mixing. By exploiting neutron tagging to muon-induced hadronic showers, spallation backgrounds in the critical 2.3–15 MeV energy range can be substantially reduced, enabling a measurement of the MSW transition with a significance $>4\sigma$ in 10 years.

Long-baseline accelerator experiments such as DUNE provide a concrete example of the importance of measuring the solar MSW transition, where JUNO alone can break degeneracies that limit their interpretation. In turn, this would provide a firm experimental foundation for next-generation measurements of the neutrino mass ordering and CP violation. The JUNO measurement could be strengthened by combining with other neutrino mixing measurements in a global analysis.

Beyond this, measuring the MSW transition would provide a model-independent calibration of matter effects, placing robust constraints on new physics that modifies neutrino propagation in matter. By doing so, a JUNO observation of the MSW transition would directly inform the interpretation of neutrino mixing across accelerator, atmospheric, and supernova experiments.

Acknowledgments.— The work of ON and JFB was supported by National Science Foundation Grant No. PHY-2310018. KJK was supported in part by Department of Energy Award No. DESC0010813.

END MATTER

Here, we provide additional details that are helpful for reproducing our results, but which are not essential for the main arguments. First, we summarize the NSI formalism. Second, we show in more detail how NSI affects the survival probability of solar neutrinos, including a brief discussion of the LMA-Dark degeneracy. Finally, we describe in detail the analysis framework.

NSI formalism.— In the presence of non-standard neutrino interactions (NSI), neutrino propagation in matter is governed by an effective matter Hamiltonian that extends the Standard Model MSW potential. Here and in the main text, we closely follow Refs. [27–29, 73]. In the flavor basis, this Hamiltonian can be written as

$$H_{\text{mat}} = \sqrt{2}G_F N_e \begin{pmatrix} 1 + \epsilon_{ee} & \epsilon_{e\mu} & \epsilon_{e\tau} \\ \epsilon_{e\mu}^* & \epsilon_{\mu\mu} & \epsilon_{\mu\tau} \\ \epsilon_{e\tau}^* & \epsilon_{\mu\tau}^* & \epsilon_{\tau\tau} \end{pmatrix}, \quad (\text{E1})$$

where the dimensionless parameters $\epsilon_{\alpha\beta}$ encode the strength of NSI relative to the Fermi constant.

In electrically neutral matter composed of electrons, protons, and neutrons, the effective NSI couplings $\epsilon_{\alpha\beta}$ can be expressed in terms of the fundamental NSI couplings to electrons, up quarks, and down quarks as

$$\epsilon_{\alpha\beta} = \epsilon_{\alpha\beta}^e + (2\epsilon_{\alpha\beta}^u + \epsilon_{\alpha\beta}^d) + \frac{N_n}{N_e}(\epsilon_{\alpha\beta}^u + 2\epsilon_{\alpha\beta}^d), \quad (\text{E2})$$

where N_e and N_n are the electron and neutron number densities, respectively.

For terrestrial experiments, the neutron density is approximately equal to the electron density, leading to an effective coupling commonly written as

$$\epsilon_{\alpha\beta}^{\oplus} \simeq \epsilon_{\alpha\beta}^e + 3\epsilon_{\alpha\beta}^u + 3\epsilon_{\alpha\beta}^d. \quad (\text{E3})$$

In contrast, in the Sun, the neutron fraction varies significantly with radius, from $Y_n \equiv N_n/N_e \simeq 0.6$ in the core to $\simeq 0.1$ near the surface. The effective solar NSI coupling can therefore be written as

$$\epsilon_{\alpha\beta}^{\odot} \simeq \epsilon_{\alpha\beta}^e + (2 + Y_n)\epsilon_{\alpha\beta}^u + (1 + 2Y_n)\epsilon_{\alpha\beta}^d. \quad (\text{E4})$$

For our calculations in the main text, we use the neutron fraction profile from standard solar models [64, 65] to evaluate the radial dependence of $\epsilon_{\alpha\beta}^{\odot}$.

For solar neutrinos, the dynamics can be well described in the two-flavor limit. Then the effective 2×2 matter Hamiltonian takes the form [27, 29, 73]

$$H_{\text{mat}} \simeq \sqrt{2}G_F N_e \begin{pmatrix} c_{13}^2 - \epsilon_D & \epsilon_N \\ \epsilon_N^* & \epsilon_D \end{pmatrix}, \quad (\text{E5})$$

where the diagonal and off-diagonal NSI parameters, ϵ_D and ϵ_N , are related to the effective couplings $\epsilon_{\alpha\beta}$ by

$$\begin{aligned} \epsilon_D &= c_{13}s_{13} \text{Re}(s_{13}\epsilon_{e\mu} + c_{23}\epsilon_{e\tau}) \\ &\quad - (1 + s_{13}^2)c_{23}s_{23} \text{Re}(\epsilon_{\mu\tau}) \\ &\quad - \frac{c_{13}^2}{2}(\epsilon_{ee} - \epsilon_{\mu\mu}) + \frac{s_{23}^2 - s_{13}^2c_{23}^2}{2}(\epsilon_{\tau\tau} - \epsilon_{\mu\mu}), \end{aligned} \quad (\text{E6})$$

$$\begin{aligned} \epsilon_N &= c_{13}(c_{23}\epsilon_{e\mu} - s_{23}\epsilon_{e\tau}) \\ &\quad + s_{13} [s_{23}^2\epsilon_{\mu\tau} - c_{23}^2\epsilon_{\mu\tau}^* + c_{23}s_{23}(\epsilon_{\tau\tau} - \epsilon_{\mu\mu})]. \end{aligned} \quad (\text{E7})$$

where $c_{ij} = \cos(\theta_{ij})$ and $s_{ij} = \sin(\theta_{ij})$.

NSI effects on the survival probability.— In the standard MSW framework, the effective matter mixing angle appearing in the Parke formula [Eq. (2)] for the survival probability is

$$\cos(2\theta_m) = \frac{\cos(2\theta_{12}) - \frac{A_{\text{CC}}}{\Delta m_{21}^2}c_{13}^2}{\sqrt{\sin^2(2\theta_{12}) + \left(\cos(2\theta_{12}) - \frac{A_{\text{CC}}}{\Delta m_{21}^2}c_{13}^2\right)^2}}, \quad (\text{E8})$$

where $A_{\text{CC}} = 2\sqrt{2}G_F N_e E_{\nu}$. At low neutrino energies or matter densities ($A_{\text{CC}}/\Delta m_{21}^2 \rightarrow 0$), the survival probability approaches a constant value, while at high neutrino energies or matter densities ($A_{\text{CC}}/\Delta m_{21}^2 \gg 1$), the survival probability approaches a different constant value. In between, the energy dependence of θ_m — as it varies from θ_{12} to $\pi/2$ — produces the characteristic MSW transition.

In the presence of NSI, the terms in the numerator and denominator of Eq. (E8) for the matter mixing angle are modified as [29, 73]

$$\cos(2\theta_{12}) \rightarrow \cos(2\theta_{12}) + \frac{2A_{\text{CC}}}{\Delta m_{21}^2}\epsilon_D, \quad (\text{E9})$$

$$\sin(2\theta_{12}) \rightarrow \sin(2\theta_{12}) + \frac{2A_{\text{CC}}}{\Delta m_{21}^2}\epsilon_N \quad (\text{E10})$$

Figure E1 illustrates the resulting distortions in the survival probability for representative values of ϵ_{ee}^{\oplus} . The three panels correspond to scenarios where ϵ_{ee}^{\oplus} arises entirely from couplings to electrons, up quarks, or down quarks. The impact is largest for the case of electron couplings, for which the mapping between terrestrial and solar NSI parameters is unity, followed by the up and down-quark cases, where the proportionality factors are reduced by $(2 + Y_n)/3$ and $(1 + 2Y_n)/3$, respectively.

The LMA-Dark degeneracy is a special but interesting NSI case [28, 31, 69, 70, 72]. Equations (E6–E10) exhibit an exact degeneracy when $\epsilon_{ee} - \epsilon_{\mu\mu} = -2$, $\epsilon_{\mu\mu} = \epsilon_{\tau\tau}$, all off-diagonal NSI parameters vanish, and the sign of Δm_{21}^2 is reversed (equivalently, when θ_{12} lies in the second octant [24, 32]). The LMA-Dark case thus cannot be separated from the standard model case using oscillation data alone. Doing so requires complementary constraints from scattering measurements. In the electron sector, this parameter space is strongly constrained by neutrino-electron and coherent elastic neutrino-nucleus scattering data for a wide range of mediator masses [69, 70, 72]. In the near future, these constraints will be further strengthened by measurements of the solar neutrino fog at dark matter experiments [32].

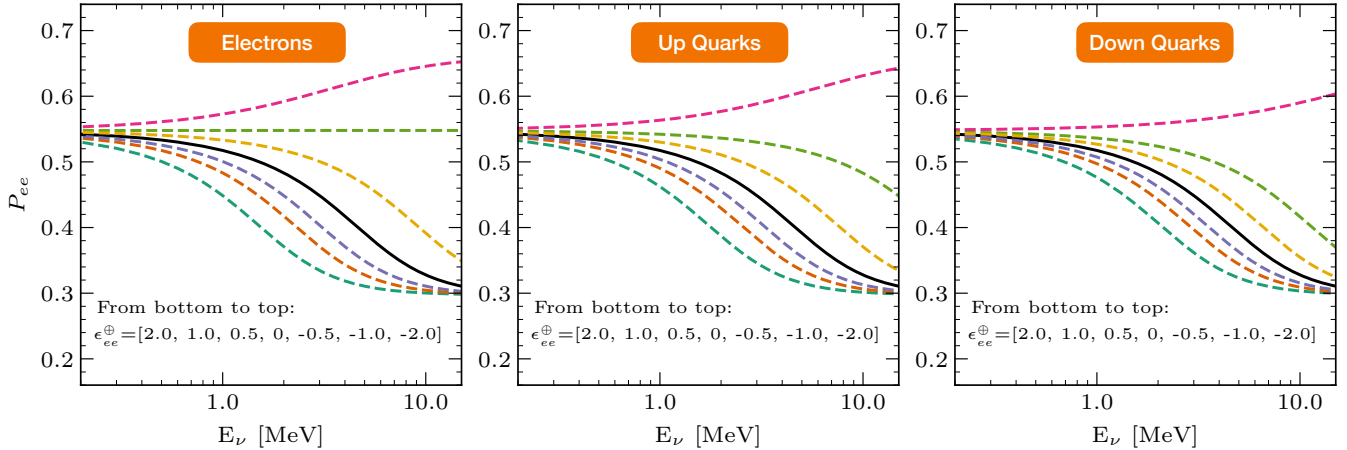


FIG. E1. Solar neutrino survival probability in the presence of NSI couplings with different fermions.

The importance of using scattering data to test NSI is more general than the LMA-Dark case alone. In our calculations, we focus on the impact of NSI on neutrino propagation, which is independent of the mediator mass. For heavy mediators, NSI can also modify the neutrino-electron scattering cross section, providing additional NSI sensitivity. In present data from Borexino, the NSI sensitivity is driven primarily by scattering data because of the lack of data in the MSW transition region. Going forward, it will be useful to use these to strengthen the sensitivity of JUNO.

Analysis details.— In evaluating JUNO’s sensitivity to the solar MSW transition, we closely follow the statistical framework in Refs. [41, 56], with some important updates motivated by recent simulation and detector performance studies.

To quantify the sensitivity, a χ^2 function is defined as

$$\chi^2 = \chi^2_{\text{data}} + \sum_j \frac{\xi_j^2}{\sigma_j^2}, \quad (\text{E11})$$

where the index j runs over the systematic uncertainties, ξ_j are the corresponding nuisance parameters, and σ_j are their errors, assumed to be Gaussian. For the data term, we use the Poisson definition,

$$\chi^2_{\text{data}} = 2 \sum_i N_{\text{flat}}^i - N_{\text{MSW}}^i + N_{\text{MSW}}^i \times \log \frac{N_{\text{MSW}}^i}{N_{\text{flat}}^i}, \quad (\text{E12})$$

where N_{flat}^i and N_{MSW}^i are the predicted event counts in the i th energy bin assuming, respectively, a flat (energy-independent) mixing probability and the standard MSW prediction. In both cases, signal and background contributions are included.

A key difference relative to Ref. [56] is that we increase the analysis threshold from 2.0 MeV to 2.3 MeV. As discussed in detail in the companion paper [58], updated FLUKA simulations indicate that the production yield of ^{13}N is larger than previously estimated. This increase might be due to improved treatment of heavy-ion transport and the inclusion of additional production channels,

such as $(^2\text{H},\text{n})$ reactions. Because ^{13}N has a long lifetime and a beta-decay endpoint at 2.2 MeV, it is particularly challenging to reduce using timing veto techniques. Raising the threshold to 2.3 MeV ensures complete removal of this background after accounting for energy smearing. While this choice leads to a modest reduction in sensitivity, it is essential to achieve a signal-dominated analysis.

The rates of the remaining spallation backgrounds are a major systematic uncertainty, due to the limited experimental measurements and significant hadronic uncertainties on the isotope yields, seen, e.g., in the different results from Geant4 and FLUKA. In Ref. [56], isotope yields were estimated by scaling measurements from previous experiments, assuming a cross section proportional to the average muon energy. (A more physical and accurate approach is to scale with shower energy [77].) That approach leads to lower yields than those obtained from our FLUKA simulations. To remain conservative, for any isotope where the two approaches disagree, we adopt the larger predicted yield and further multiply it by a factor of two, consistent with the typical level of hadronic uncertainty.

For all remaining background components, we adopt the rates and uncertainties from Ref. [56], except in cases where updated measurements are available from JUNO’s recent initial detector performance studies. In those instances, we use the experimentally measured values and their associated uncertainties. Altogether, this results in approximately 5×10^4 background events in a 10-year exposure, compared to about 3×10^4 events in Ref. [56], providing a conservative estimate of JUNO’s sensitivity.

Systematic uncertainties associated with the energy scale and the shape of the ^8B neutrino spectrum are treated following the procedure of Ref. [56], by introducing energy-dependent shift parameters applied to the predicted spectra. The detector energy resolution is taken to be 3% at 1 MeV. We have verified that increasing the resolution to 5% has a negligible impact on the main results presented in this work.

* nairat.2@osu.edu
 † beacom.7@osu.edu
 ‡ kjkelly@tamu.edu
 § shirley.li@uci.edu

[1] Y. Fukuda *et al.* (Super-Kamiokande), Evidence for oscillation of atmospheric neutrinos, *Phys. Rev. Lett.* **81**, 1562 (1998), [arXiv:hep-ex/9807003](#).

[2] S. Fukuda *et al.* (Super-Kamiokande), Solar B-8 and hep neutrino measurements from 1258 days of Super-Kamiokande data, *Phys. Rev. Lett.* **86**, 5651 (2001), [arXiv:hep-ex/0103032](#).

[3] K. Abe *et al.* (Super-Kamiokande), Solar neutrino results in Super-Kamiokande-III, *Phys. Rev. D* **83**, 052010 (2011), [arXiv:1010.0118 \[hep-ex\]](#).

[4] K. Abe *et al.* (Super-Kamiokande), Solar Neutrino Measurements in Super-Kamiokande-IV, *Phys. Rev. D* **94**, 052010 (2016), [arXiv:1606.07538 \[hep-ex\]](#).

[5] Q. R. Ahmad *et al.* (SNO), Direct evidence for neutrino flavor transformation from neutral current interactions in the Sudbury Neutrino Observatory, *Phys. Rev. Lett.* **89**, 011301 (2002), [arXiv:nucl-ex/0204008](#).

[6] B. Aharmim *et al.* (SNO), Combined Analysis of all Three Phases of Solar Neutrino Data from the Sudbury Neutrino Observatory, *Phys. Rev. C* **88**, 025501 (2013), [arXiv:1109.0763 \[nucl-ex\]](#).

[7] K. Eguchi *et al.* (KamLAND), First results from KamLAND: Evidence for reactor anti-neutrino disappearance, *Phys. Rev. Lett.* **90**, 021802 (2003), [arXiv:hep-ex/0212021](#).

[8] S. Abe *et al.* (KamLAND), Precision Measurement of Neutrino Oscillation Parameters with KamLAND, *Phys. Rev. Lett.* **100**, 221803 (2008), [arXiv:0801.4589 \[hep-ex\]](#).

[9] G. Bellini *et al.* (Borexino), First evidence of pep solar neutrinos by direct detection in Borexino, *Phys. Rev. Lett.* **108**, 051302 (2012), [arXiv:1110.3230 \[hep-ex\]](#).

[10] M. Agostini *et al.* (BOREXINO), Comprehensive measurement of pp -chain solar neutrinos, *Nature* **562**, 505 (2018).

[11] X. Guo *et al.* (Daya Bay), A Precision measurement of the neutrino mixing angle θ_{13} using reactor antineutrinos at Daya-Bay, (2007), [arXiv:hep-ex/0701029](#).

[12] F. P. An *et al.* (Daya Bay), Observation of electron-antineutrino disappearance at Daya Bay, *Phys. Rev. Lett.* **108**, 171803 (2012), [arXiv:1203.1669 \[hep-ex\]](#).

[13] L. Wolfenstein, Neutrino Oscillations in Matter, *Phys. Rev. D* **17**, 2369 (1978).

[14] S. P. Mikheyev and A. Y. Smirnov, Resonance Amplification of Oscillations in Matter and Spectroscopy of Solar Neutrinos, *Sov. J. Nucl. Phys.* **42**, 913 (1985).

[15] J. F. Beacom and P. Vogel, Neutrino magnetic moments, flavor mixing, and the Super-Kamiokande solar data, *Phys. Rev. Lett.* **83**, 5222 (1999), [arXiv:hep-ph/9907383](#).

[16] J. F. Beacom and N. F. Bell, Do Solar Neutrinos Decay?, *Phys. Rev. D* **65**, 113009 (2002), [arXiv:hep-ph/0204111](#).

[17] A. Friedland, C. Lunardini, and C. Pena-Garay, Solar neutrinos as probes of neutrino matter interactions, *Phys. Lett. B* **594**, 347 (2004), [arXiv:hep-ph/0402266](#).

[18] J. M. Berryman, A. de Gouvea, and D. Hernandez, Solar Neutrinos and the Decaying Neutrino Hypothesis, *Phys. Rev. D* **92**, 073003 (2015), [arXiv:1411.0308 \[hep-ph\]](#).

[19] M. Maltoni and A. Y. Smirnov, Solar neutrinos and neutrino physics, *Eur. Phys. J. A* **52**, 87 (2016), [arXiv:1507.05287 \[hep-ph\]](#).

[20] Y. Farzan and M. Tortola, Neutrino oscillations and Non-Standard Interactions, *Front. in Phys.* **6**, 10 (2018), [arXiv:1710.09360 \[hep-ph\]](#).

[21] G.-Y. Huang and S. Zhou, Constraining Neutrino Lifetimes and Magnetic Moments via Solar Neutrinos in the Large Xenon Detectors, *JCAP* **02**, 024, [arXiv:1810.03877 \[hep-ph\]](#).

[22] *Neutrino Non-Standard Interactions: A Status Report*, Vol. 2 (2019) [arXiv:1907.00991 \[hep-ph\]](#).

[23] M. Hostert and M. Pospelov, Constraints on decaying sterile neutrinos from solar antineutrinos, *Phys. Rev. D* **104**, 055031 (2021), [arXiv:2008.11851 \[hep-ph\]](#).

[24] P. B. Denton and S. J. Parke, Parameter symmetries of neutrino oscillations in vacuum, matter, and approximation schemes, *Phys. Rev. D* **105**, 013002 (2022), [arXiv:2106.12436 \[hep-ph\]](#).

[25] K. Goldhagen, M. Maltoni, S. E. Reichard, and T. Schwetz, Testing sterile neutrino mixing with present and future solar neutrino data, *Eur. Phys. J. C* **82**, 116 (2022), [arXiv:2109.14898 \[hep-ph\]](#).

[26] C. A. Argüelles *et al.*, Snowmass white paper: beyond the standard model effects on neutrino flavor: Submitted to the proceedings of the US community study on the future of particle physics (Snowmass 2021), *Eur. Phys. J. C* **83**, 15 (2023), [arXiv:2203.10811 \[hep-ph\]](#).

[27] P. Coloma, M. C. Gonzalez-Garcia, M. Maltoni, J. P. Pinheiro, and S. Urrea, Constraining new physics with Borexino Phase-II spectral data, *JHEP* **07**, 138, [Erratum: JHEP 11, 138 (2022)], [arXiv:2204.03011 \[hep-ph\]](#).

[28] P. Coloma, M. C. Gonzalez-Garcia, M. Maltoni, J. P. Pinheiro, and S. Urrea, Global constraints on non-standard neutrino interactions with quarks and electrons, *JHEP* **08**, 032, [arXiv:2305.07698 \[hep-ph\]](#).

[29] D. W. P. Amaral, D. Cerdeno, A. Cheek, and P. Foldenauer, A direct detection view of the neutrino NSI landscape, *JHEP* **07**, 071, [arXiv:2302.12846 \[hep-ph\]](#).

[30] P. B. Denton, A. Giannetti, and D. Meloni, Solar neutrinos and the strongest oscillation constraints on scalar NSI, *JHEP* **01**, 097, [arXiv:2409.15411 \[hep-ph\]](#).

[31] S. Chattopadhyay and A. Dighe, Refractive neutrino masses in the solar DM halo: Can the dark-LMA solution be revived?, (2025), [arXiv:2511.19420 \[hep-ph\]](#).

[32] J. Gehrlein and T. Kushwaha, Testing the dark side of neutrino oscillations with the solar neutrino fog at dark matter experiments, *Phys. Rev. D* **112**, 095032 (2025), [arXiv:2508.14166 \[hep-ph\]](#).

[33] K. Abe *et al.* (T2K), Improved constraints on neutrino mixing from the T2K experiment with 3.13×10^{21} protons on target, *Phys. Rev. D* **103**, 112008 (2021), [arXiv:2101.03779 \[hep-ex\]](#).

[34] M. A. Acero *et al.* (NOvA), Improved measurement of neutrino oscillation parameters by the NOvA experiment, *Phys. Rev. D* **106**, 032004 (2022), [arXiv:2108.08219 \[hep-ex\]](#).

[35] R. Abbasi *et al.* (IceCube), All-flavor constraints on non-standard neutrino interactions and generalized matter potential with three years of IceCube DeepCore data, *Phys. Rev. D* **104**, 072006 (2021), [arXiv:2106.07755 \[hep-ex\]](#).

[36] T. Wester *et al.* (Super-Kamiokande), Atmospheric neutrino oscillation analysis with neutron tagging and an expanded fiducial volume in Super-Kamiokande I–V, *Phys. Rev. D* **109**, 072014 (2024), arXiv:2311.05105 [hep-ex].

[37] S. Abubakar *et al.* (T2K, NOvA), Joint neutrino oscillation analysis from the T2K and NOvA experiments, *Nature* **646**, 818 (2025), arXiv:2510.19888 [hep-ex].

[38] W. C. Haxton, R. G. Hamish Robertson, and A. M. Serenelli, Solar Neutrinos: Status and Prospects, *Ann. Rev. Astron. Astrophys.* **51**, 21 (2013), arXiv:1208.5723 [astro-ph.SR].

[39] G. D. O. Gann, K. Zuber, D. Bemmerer, and A. Serenelli, The Future of Solar Neutrinos, *Ann. Rev. Nucl. Part. Sci.* **71**, 491 (2021), arXiv:2107.08613 [hep-ph].

[40] X.-J. Xu, Z. Wang, and S. Chen, Solar neutrino physics, *Prog. Part. Nucl. Phys.* **131**, 104043 (2023), arXiv:2209.14832 [hep-ph].

[41] K. Abe *et al.* (Super-Kamiokande), Solar neutrino measurements using the full data period of Super-Kamiokande-IV, *Phys. Rev. D* **109**, 092001 (2024), arXiv:2312.12907 [hep-ex].

[42] B. Abi *et al.* (DUNE), Deep Underground Neutrino Experiment (DUNE), Far Detector Technical Design Report, Volume I Introduction to DUNE, *JINST* **15** (08), T08008, arXiv:2002.02967 [physics.ins-det].

[43] B. Abi *et al.* (DUNE), Deep Underground Neutrino Experiment (DUNE), Far Detector Technical Design Report, Volume II: DUNE Physics, (2020), arXiv:2002.03005 [hep-ex].

[44] P. Coloma, Non-Standard Interactions in propagation at the Deep Underground Neutrino Experiment, *JHEP* **03**, 016, arXiv:1511.06357 [hep-ph].

[45] A. de Gouv  a and K. J. Kelly, Non-standard neutrino interactions at DUNE, *Nucl. Phys. B* **908**, 318 (2016), arXiv:1511.05562 [hep-ph].

[46] A. de Gouv  a and K. J. Kelly, False Signals of CP-Invariance Violation at DUNE, (2016), arXiv:1605.09376 [hep-ph].

[47] J. Liao, D. Marfatia, and K. Whisnant, Nonstandard neutrino interactions at DUNE, T2HK and T2HKK, *JHEP* **01**, 071, arXiv:1612.01443 [hep-ph].

[48] K. Abe *et al.* (Hyper-Kamiokande), Hyper-Kamiokande Design Report, (2018), arXiv:1805.04163 [physics.ins-det].

[49] K. J. Kelly, P. A. N. Machado, I. Martinez-Soler, and Y. F. Perez-Gonzalez, DUNE atmospheric neutrinos: Earth tomography, *JHEP* **05**, 187, arXiv:2110.00003 [hep-ph].

[50] J. Bian *et al.* (Hyper-Kamiokande), Hyper-Kamiokande Experiment: A Snowmass White Paper, in *Snowmass 2021* (2022) arXiv:2203.02029 [hep-ex].

[51] H. Duan, G. M. Fuller, J. Carlson, and Y.-Z. Qian, Simulation of Coherent Non-Linear Neutrino Flavor Transformation in the Supernova Environment. 1. Correlated Neutrino Trajectories, *Phys. Rev. D* **74**, 105014 (2006), arXiv:astro-ph/0606616.

[52] H. Duan, G. M. Fuller, and Y.-Z. Qian, Collective Neutrino Oscillations, *Ann. Rev. Nucl. Part. Sci.* **60**, 569 (2010), arXiv:1001.2799 [hep-ph].

[53] S. Chakraborty, R. S. Hansen, I. Izaguirre, and G. Raafelt, Self-induced neutrino flavor conversion without flavor mixing, *JCAP* **03**, 042, arXiv:1602.00698 [hep-ph].

[54] A. Capanema, Y. Porto, and M. M. Saez, Flavor composition of supernova neutrinos, *Phys. Rev. D* **111**, 103021 (2025), arXiv:2403.14762 [hep-ph].

[55] F. An *et al.* (JUNO), Neutrino Physics with JUNO, *J. Phys. G* **43**, 030401 (2016), arXiv:1507.05613 [physics.ins-det].

[56] A. Abusleme *et al.* (JUNO), Feasibility and physics potential of detecting ^8B solar neutrinos at JUNO, *Chin. Phys. C* **45**, 023004 (2021), arXiv:2006.11760 [hep-ex].

[57] A. Abusleme *et al.* (JUNO), First measurement of reactor neutrino oscillations at JUNO, (2025), arXiv:2511.14593 [hep-ex].

[58] O. Nairat, J. F. Beacom, and S. W. Li, New Spallation Background Rejection Techniques to Greatly Improve the Solar Neutrino Sensitivity of JUNO, (2025), arXiv:2510.12873 [hep-ph].

[59] C. Giunti and C. W. Kim, *Fundamentals of Neutrino Physics and Astrophysics* (2007).

[60] P. B. Denton, Neutrino Oscillations in the Three Flavor Paradigm, (2025), arXiv:2501.08374 [hep-ph].

[61] S. Navas *et al.* (Particle Data Group), Review of particle physics, *Phys. Rev. D* **110**, 030001 (2024).

[62] A. N. Khan, H. Nunokawa, and S. J. Parke, Why matter effects matter for JUNO, *Phys. Lett. B* **803**, 135354 (2020), arXiv:1910.12900 [hep-ph].

[63] S. J. Parke, Nonadiabatic Level Crossing in Resonant Neutrino Oscillations, *Phys. Rev. Lett.* **57**, 1275 (1986), arXiv:2212.06978 [hep-ph].

[64] J. N. Bahcall, A. M. Serenelli, and S. Basu, New solar opacities, abundances, helioseismology, and neutrino fluxes, *Astrophys. J. Lett.* **621**, L85 (2005), arXiv:astro-ph/0412440.

[65] J. N. Bahcall, A. M. Serenelli, and S. Basu, 10,000 standard solar models: a Monte Carlo simulation, *Astrophys. J. Suppl.* **165**, 400 (2006), arXiv:astro-ph/0511337.

[66] P. B. Denton and C. Gourley, Determining the density of the sun with neutrinos, *Phys. Lett. B* **866**, 139560 (2025), arXiv:2502.17546 [hep-ph].

[67] M. A. Zaidel and J. F. Beacom, Probing the conditions of the solar core using $B8$ neutrinos, *Phys. Rev. C* **112**, 055801 (2025), arXiv:2504.10583 [astro-ph.SR].

[68] I. Esteban, M. C. Gonzalez-Garcia, M. Maltoni, I. Martinez-Soler, J. P. Pinheiro, and T. Schwetz, NuFit-6.0: updated global analysis of three-flavor neutrino oscillations, *JHEP* **12**, 216, arXiv:2410.05380 [hep-ph].

[69] P. Coloma, P. B. Denton, M. C. Gonzalez-Garcia, M. Maltoni, and T. Schwetz, Curtailing the Dark Side in Non-Standard Neutrino Interactions, *JHEP* **04**, 116, arXiv:1701.04828 [hep-ph].

[70] P. B. Denton, Y. Farzan, and I. M. Shoemaker, Testing large non-standard neutrino interactions with arbitrary mediator mass after COHERENT data, *JHEP* **07**, 037, arXiv:1804.03660 [hep-ph].

[71] N. Bernal and Y. Farzan, Neutrino nonstandard interactions with arbitrary couplings to u and d quarks, *Phys. Rev. D* **107**, 035007 (2023), arXiv:2211.15686 [hep-ph].

[72] P. B. Denton and J. Gehrlein, New constraints on the dark side of non-standard interactions from reactor neutrino scattering data, *Phys. Rev. D* **106**, 015022 (2022), arXiv:2204.09060 [hep-ph].

[73] A. C. Shekar, C. Lisotti, N. Mishra, C. A. J. O'Hare, and L. E. Strigari, Searching for beyond-standard-model solar neutrino interactions using directional detectors, *Phys. Rev. D* **112**, 123021 (2025), arXiv:2506.09322 [hep-ph].

[74] A. Abusleme *et al.* (JUNO), Initial performance results of the JUNO detector, (2025), arXiv:2511.14590 [hep-ex].

[75] J. Zhao *et al.* (JUNO), Model-independent Approach of the JUNO ${}^8\text{B}$ Solar Neutrino Program, *Astrophys. J.* **965**, 122 (2024), arXiv:2210.08437 [hep-ex].

[76] S. W. Li and J. F. Beacom, First calculation of cosmic-ray muon spallation backgrounds for MeV astrophysical neutrino signals in Super-Kamiokande, *Phys. Rev. C* **89**, 045801 (2014), arXiv:1402.4687 [hep-ph].

[77] S. W. Li and J. F. Beacom, Spallation Backgrounds in Super-Kamiokande Are Made in Muon-Induced Showers, *Phys. Rev. D* **91**, 105005 (2015), arXiv:1503.04823 [hep-ph].

[78] S. W. Li and J. F. Beacom, Tagging Spallation Backgrounds with Showers in Water-Cherenkov Detectors, *Phys. Rev. D* **92**, 105033 (2015), arXiv:1508.05389 [physics.ins-det].

[79] O. Nairat, J. F. Beacom, and S. W. Li, Neutron tagging can greatly reduce spallation backgrounds in Super-Kamiokande, *Phys. Rev. D* **111**, 023014 (2025), arXiv:2409.10611 [hep-ph].

[80] G. Zhu, S. W. Li, and J. F. Beacom, Developing the MeV potential of DUNE: Detailed considerations of muon-induced spallation and other backgrounds, *Phys. Rev. C* **99**, 055810 (2019), arXiv:1811.07912 [hep-ph].

[81] W. T. Winter, S. J. Freedman, K. E. Rehm, and J. P. Schiffer, The B-8 neutrino spectrum, *Phys. Rev. C* **73**, 025503 (2006), arXiv:nucl-ex/0406019.

[82] J. N. Bahcall, M. Kamionkowski, and A. Sirlin, Solar neutrinos: Radiative corrections in neutrino - electron scattering experiments, *Phys. Rev. D* **51**, 6146 (1995), arXiv:astro-ph/9502003.

[83] A. Li, A. Elagin, S. Fraker, C. Grant, and L. Winslow, Suppression of Cosmic Muon Spallation Backgrounds in Liquid Scintillator Detectors Using Convolutional Neural Networks, *Nucl. Instrum. Meth. A* **947**, 162604 (2019), arXiv:1812.02906 [physics.ins-det].

[84] X. Zhang, H. Lu, C. Yang, Z. Yu, and Y. Wang, A novel discrimination method for neutrinos and cosmogenic isotopes in liquid scintillator-based detectors, *Radiat. Detect. Technol. Methods* **8**, 1448 (2024).

[85] K. N. Deepthi, S. Goswami, and N. Nath, Can non-standard interactions jeopardize the hierarchy sensitivity of DUNE?, *Phys. Rev. D* **96**, 075023 (2017), arXiv:1612.00784 [hep-ph].

[86] I. Esteban, M. C. Gonzalez-Garcia, and M. Maltoni, On the Determination of Leptonic CP Violation and Neutrino Mass Ordering in Presence of Non-Standard Interactions: Present Status, *JHEP* **06**, 055, arXiv:1905.05203 [hep-ph].

[87] F. Capozzi, S. S. Chatterjee, and A. Palazzo, Neutrino Mass Ordering Obscured by Nonstandard Interactions, *Phys. Rev. Lett.* **124**, 111801 (2020), arXiv:1908.06992 [hep-ph].

[88] S.-F. Ge and A. Y. Smirnov, Non-standard interactions and the CP phase measurements in neutrino oscillations at low energies, *JHEP* **10**, 138, arXiv:1607.08513 [hep-ph].

[89] P. B. Denton, J. Gehrlein, and R. Pestes, *CP* -Violating Neutrino Nonstandard Interactions in Long-Baseline-Accelerator Data, *Phys. Rev. Lett.* **126**, 051801 (2021), arXiv:2008.01110 [hep-ph].

[90] S. S. Chatterjee and A. Palazzo, Nonstandard Neutrino Interactions as a Solution to the *NOvA* and T2K Discrepancy, *Phys. Rev. Lett.* **126**, 051802 (2021), arXiv:2008.04161 [hep-ph].

[91] M. A. Acero *et al.* (NOvA), Search for CP-Violating Neutrino Nonstandard Interactions with the NOvA Experiment, *Phys. Rev. Lett.* **133**, 201802 (2024), arXiv:2403.07266 [hep-ex].